







Land-Cover Mapping in the Biogradska Gora National Park with Very-High-Resolution Pléiades Images

Eleonora Cagliero^{1,2}  , Donato Morresi³ , Niccolò Marchi¹ ,
Laure Paradis² , Walter Finsinger² , Matteo Garbarino³ ,
and Emanuele Lingua¹ 

¹ Department of Land, Environment, Agriculture and Forestry (TESAF),
University of Padova, 35020 Legnaro, PD, Italy
eleonora.cagliero@phd.unipd.it

² University of Montpellier, ISEM, CNRS, IRD, EPHE, Montpellier, France

³ Department of Agricultural, Forest and Food Sciences (DISAFA),
University of Torino, 10095 Grugliasco, TO, Italy

Abstract. Old-growth forests (OGFs) are extremely valuable relict ecosystems for studying natural disturbance dynamics. Small-scale disturbances caused by tree crown mortality of one or few individuals, i.e. gap dynamics, are the most frequent events occurring in OGFs. Understanding these processes requires information on the spatial arrangement of forest patches dominated by different tree species and forest canopy gaps at a fine spatial scale. Here, we aimed at mapping different land-cover classes including conifers, broad-leaved trees, and forest canopy gaps using two very-high-resolution satellite images, i.e. Pléiades images, in the mixed fir-spruce-beech OGF reserve of Biogradska Gora (Montenegro). Specifically, we coupled an Object-Based Image Analysis (OBIA) approach and a Random Forest classifier, trained with samples partly derived from field data. The adopted approach showed high accuracy for the main land-cover classes (conifers, broadleaved trees, grasslands, bare ground, and water), e.g. producer's and user's accuracy higher than 92% and 95%, respectively. Conversely, forest canopy gaps were classified with lower accuracy, e.g. minimum producer's and user's accuracies of 75% and 54%, respectively. Despite the exploitation of textural metrics during both image segmentation and classification, the lack of remote sensing data providing information on the vertical structure of the forest stand prevented us from accurately map forest canopy gaps.

Keyword: Very-high-resolution satellite imagery · Old-growth forest · Land-cover map · Object-based image analysis · Forest canopy gaps

1 Introduction

Old-growth forests (OGFs) are ecosystems that have developed in the absence of anthropogenic influence and of stand-replacing natural disturbances for a period of time long

enough (centuries-millennia) to develop peculiar structures and functions [1]. OGFs provide a wide range of ecosystem services, contributing to global biodiversity conservation and to mitigate climate change by carbon sequestration [1]. Moreover, OGFs act as reference systems for restoration and close-to-nature silviculture [2] because vegetation dynamics take place without direct human influence.

Depending on the predominant dynamics, OGFs have structural characteristics that vary among geographic areas. In temperate forests, large-scale natural disturbances are rare, and the stand dynamics are mainly characterized by small- to intermediate-scale forest canopy openings (gap dynamics) following the natural- or disturbances-caused mortality of single or small groups of dominant forest canopy trees [3]. The temporal and spatial interplay of type, size and frequency of disturbance events influences the species composition of the canopy layer and determines the creation of a heterogeneous mosaic of structural types [4] that is particularly developed in large OGFs (> 1000 ha). However, presumably due to widespread millennial-long and increasing rates of land-use change [5, 6], large OGFs are rare today in Europe and mainly located in protected areas [6].

In the last decades, forest stand dynamics have been investigated mostly with terrestrial methods, such as representative sample plots (permanent or not), extensive field surveys, belt transects, and systematic grids [4, 7–10]. However, the structural heterogeneity of OGFs require a finer scale of analysis than terrestrial methods, which are expensive [11] and time-consuming, especially in OGFs, as these often are in remote places and difficult to access.

In this context, coupling remote sensing methods with field data as ground-control [3] is particularly valuable since it allows analyzing patterns (e.g. land-cover maps) and processes (e.g. gap dynamics) at the landscape scale in a shorter amount of time [3, 12, 13]. Moreover, remote sensing allows performing multi-temporal analyses to assess forest cover changes through time [14]. For instance, the extent and number of gaps continuously change due to (i) the formation of new ones and (ii) infilling by young trees and (iii) the expansion of older gaps. Even if the temporal dynamics can be deduced from field-based methods (by dendrochronology or repeated inventory in permanent plots), remote sensing analyses based on satellite imagery would be more cost-effective and could provide spatial information over broad areas.

However, the detection of fine-scale forest components, such as tree crowns and small forest canopy gaps, is constrained by the availability of very-high-resolution (c. <5 m) multispectral satellite imagery (e.g. Ikonos, Pléiades, QuickBird, Kompsat-2, WorldView-2) [3, 15]. To our knowledge, only few studies employed single very-high-spatial-resolution satellite images for mapping forest canopy gaps [3] while others took advantage of stereo aerial imagery [16] or integrated multispectral and LiDAR data [15]. Given the smaller pixel dimension with respect to the image objects of interest, a common approach adopted with high-spatial-resolution imagery is to perform Object-Based Image Analysis (OBIA) [17]. This technique aims at grouping neighboring image pixels with similar spectral and textural characteristics into objects, thus reducing their internal variability. OBIA avoids the “salt and pepper” noise commonly resulting in the classification compared to the traditional pixel-based methods and aims at delineating image objects that closely correspond to the size and the shape of real features [18].

Here we focused on the Biogradska Gora mixed beech-fir-spruce OGF (Montenegro), a forest landscape large enough to develop the whole natural temporal and spatial variability of forest dynamics [5]. Specifically, we aimed at mapping different land-cover classes including conifers, broad-leaved trees, and forest canopy gaps, using two very-high-resolution Pléiades images and coupling OBIA and a Random Forest classifier.

2 Methodology

2.1 Study Site

The Biogradska Gora National Park (Fig. 1) is located in the Dinaric Alps. The reserve area of the park (c. 6000 ha) includes a core area of strict protection of c. 2830 ha surrounded by a buffer zone (Fig. 1). In the core area, all land-use activities are prohibited except scientific research and controlled tourism. Instead, pastoral farming is allowed in the buffer zone, as meadows and shepherds' huts testimony. The reserve area is protected since 1885 CE as royal hunting reserve and since 1950 when the National Park was established. The climate is characterized by a mean annual temperature of c. 7 °C, and an annual average precipitation of 1962 mm with maximum values in November-December and minimum values in July-August. In the reserve area the overstorey is dominated by European beech, silver fir, and Norway spruce with lesser amounts of other tree species such as maples, common ash, and elms [5].

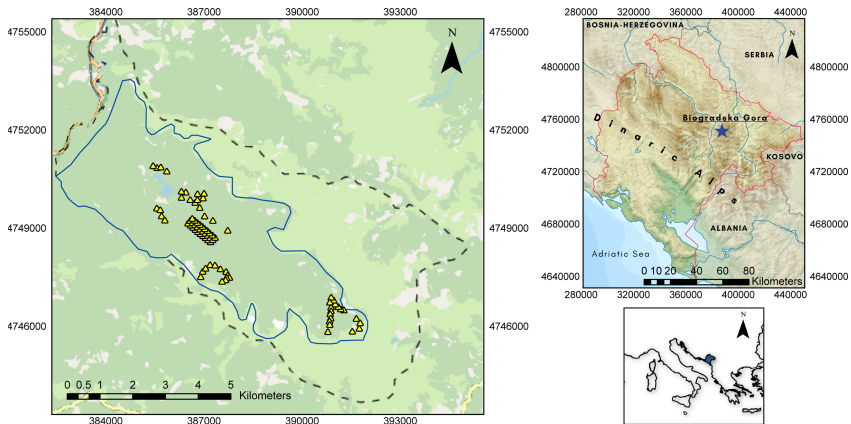


Fig. 1. Maps of the location of the study site at decreasing spatial scales and of the 81 forest plots (yellow triangles). Delimitation of the administrative boundary of Montenegro (red continuous line), of the reserve area (black dashed line) and of the core area of the Biogradska Gora National Park (blue continuous line). Reference system EPSG:32634 (WGS 84/UTM zone 34N). (Color figure online)

2.2 Field Surveys

To characterize the forest structure and the tree-species composition and to obtain ground control points for remote sensing analyses, we carried out field campaigns in May and

September 2019. We defined the location of the 51 survey plots (Fig. 1) using a forest map produced by Motta et al. [5] obtained by the classification of a SPOT5 image (acquired in May 2007) adopting an unsupervised classification algorithm (ISODATA) on three multispectral bands (G, R, and NIR). In each circular plot (area = 615.5 m²; radius = 14 m) for all the living trees with a diameter at 1.30 m (DBH) \geq 7.5 cm we recorded the species and DBH and for a sub-sample of individuals belonging to different species and diametrical classes we measured the height. We then measured the minimum and the maximum diameter and the length of the coarse woody debris (CWD) to assess the volume of dead biomass. We pooled the data of our 51 plots with the data of 30 plots surveyed by Motta et al. [5] in a 120-m grid network adopting the same field protocol. For each of the resulting 81 plots we derived typical forest stand parameters, such as mean and standard deviation of DBH, total tree density (De), and basal area (BA). We inferred the unmeasured tree heights using specie-specific hypsometric curves that we built based on the field data and computed the volume of living trees (V) using a local volume table.

2.3 Image Pre-processing

To map the distribution of six land-cover classes (conifer trees, broadleaved trees, grasslands-meadows, forest canopy gaps, bare ground, and water), we did an Object-Based Image Analysis (OBIA) on two very-high-resolution satellite images. Specifically, we used two Pléiades images (1A and 1B) acquired during the growing season of two subsequent years: on the 30th of August 2015 and on the 1st of August 2016, respectively. The images are spatially complementary, as the footprint of the 2015 image misses the upper part of the basin while the 2016 one was partly covered by clouds and cloud shadows over the forested area. The Pléiades images were provided already orthorectified and included a 0.5-m panchromatic band (PAN) and four 2-m resolution multispectral bands (RGB and NIR). We used the nearest neighbour diffusion (NNDiffuse) algorithm [19] to pan-sharpen the multispectral bands. The images were then co-registered in ENVI version 5.3.1 (Exelis Visual Information Solutions, Boulder, Colorado), using the Bing satellite image as reference. Subsequently, we masked invalid pixels, i.e. clouds and cloud shadows, through on-screen digitization.

2.4 Image Segmentation and Classification

We obtained image objects representing small groups of crowns using the Large-Scale Mean-Shift (LSMS) segmentation algorithm [20] implemented in Orfeo ToolBox version 7.0 [21] (Fig. 4). In particular, we set the following parameters in the LSMS algorithm: a spatial radius of 20 pixels, a range radius of 0.015 (as all rasters in the input stack assumed values ranging from 0 to 1) and a minimum region size of 200 pixels. We employed the Normalized Difference Vegetation Index (NDVI), the near-infrared band (NIR), and textural data derived from the mathematical morphology technique called opening as input rasters in the LSMS segmentation procedure. The opening procedure involves an erosion operation followed by dilation using a 2-dimensional structuring element (SE) [22], and it is applied to grey values of an image to eliminate objects smaller than the SE. Specifically, we used a 7-pixel diameter disc (corresponding to 3.5 m) as SE because this

shape and size performed well to the smallest tree crowns recognizable in the Pléiades images. We performed the opening operation using grey values relative to the Value component of the Hue-Saturation-Value (HSV) transformation, which we applied to the red, green and blue bands of the Pleiades images. Since the Value component corresponds to the brightness of a surface, the opening procedure allowed us to maximize the contrast between sunlit crowns, generally located at the top of the forest stand, and darker portions in the background, corresponding to shorter trees and canopy gaps. We employed the Random Forest (RF) algorithm [23] implemented in the ‘ranger’ [24] R package (R Core Team 2019) to perform a supervised classification of the image objects. We created a set of 1457 training samples evenly distributed over the study area and stratified by land-cover class (Table 1) through on-screen photointerpretation of image objects intersecting the ground forest plots (groups of broadleaved trees, groups of conifer trees, forest canopy gaps) and of objects we did not survey (grasslands-meadows, bare ground and water). Predictor variables used in the RF classifier included several textural metrics together with reflectance values and selected spectral vegetation indices (Table 2).

We assessed the classification accuracy through a 5-fold cross-validation procedure and we analyzed each Pléiades image separately, merging classification results to obtain a unique land-cover map for the whole study area.

Since forest canopy gaps are areas temporary without a tree canopy cover (due to natural disturbances, gap dynamics), all the gaps permanently without tree vegetation due to limiting factors to tree growth (e.g. edaphic conditions, shallow water table) or human activities (e.g. pastures) that were erroneously classified as forest canopy gaps were filtered out in QGIS by a topological query before computing the number of gaps, size statistics and the gap fraction [25].

Table 1. Number of training samples in each land-cover class.

| Class | Training samples | | TOT |
|--------------------|---------------------------------|--------------------------------|-----|
| | Image acquisition | | |
| | 30 th of August 2015 | 1 st of August 2016 | |
| Conifer trees | 611 | 93 | 704 |
| Broadleaved trees | 435 | 137 | 572 |
| Forest canopy gaps | 18 | 11 | 29 |
| Grasslands | 66 | 19 | 85 |
| Bare ground | 32 | 27 | 59 |
| Water | 8 | – | 8 |

3 Results

The Biogradska Gora mixed fir-spruce-beech forest is characterized by the presence of large trees (DBH up to 150 cm, average DBH = 33.89 cm), and high volume of

Table 2. Details concerning the spectral and textural layers used to compute multiple summary statistics employed as predictor variables in the Random Forest (RF) model. NDVI = Normalized Difference Vegetation Index; EVI = Enhanced Vegetation Index; GNDVI = Green Normalized Difference Vegetation Index; MSAVI = Modified Soil Adjusted Vegetation Index; NDWI = Normalized Difference Water Index; SAVI = Soil Adjusted Vegetation Index; SR = Simple Ratio.

| Spectral and textural layers | Summary statistics |
|--|--|
| Pléiades reflectance bands (PAN and MS) | Min; max; range; sum; |
| Spectral vegetation indices (NDVI; EVI; GNDVI; MSAVI; NDWI; SAVI; SR) | mean; variance; Gini |
| Morphological opening (kernels widths: 3; 5; 7; 9; 11; 13) | coefficient; standard |
| Simple Haralick textures (Energy; Entropy; Correlation; Inverse Difference Moment; Inertia; Cluster Shade; Cluster Prominence; Haralick Correlation) | deviation; percentiles (5 th , 25 th , 50 th , 75 th , 95 th) |

both living (907.3 m³/ha) and dead biomass (251.57 m³/ha). The forest stands show a complex horizontal and vertical structure, a high tree size diversification (DBH standard deviation of 22.74 cm), and a rotated sigmoidal DBH distribution.

The land-cover map derived from the Pléiades images (Fig. 2) confirmed on a small scale the spatial heterogeneity of the forest canopy. The overall good performance of the classifier is shown by high values of K and OA (Table 3). However, the classification accuracy differed greatly among classes. The Random Forest classifier performed better (in terms of both PA and UA) for conifers, broadleaved trees, grasslands, bare ground, and water classes while its accuracy was substantially lower for forest canopy gaps (Table 3).

Table 3. RF classification accuracy as assessed by means of overall (OA) and Cohen's Kappa (K) accuracies. Producer's (PA) and User's (UA) accuracies are grouped by land-cover classes.

| Class | Image acquisition | | | |
|--------------------|---------------------------------|-------|--------------------------------|-------|
| | 30 th of August 2015 | | 1 st of August 2016 | |
| | PA | UA | PA | UA |
| Conifer trees | 95.8 | 96.1 | 92.9 | 97.8 |
| Broadleaved trees | 95.2 | 95.6 | 98.5 | 97.8 |
| Forest canopy gaps | 75.0 | 66.7 | 100.0 | 54.5 |
| Grasslands | 100.0 | 97.0 | 100.0 | 100.0 |
| Bare ground | 100.0 | 100.0 | 96.4 | 100.0 |

(continued)

According to the image classification (Fig. 2), the majority of the reserve area (61.09%) is covered by forest, followed by 33.56% of grasslands, 3.94% of bare ground,

Table 3. (continued)

| Class | Image acquisition | | | |
|-------|---------------------------------|-------|--------------------------------|------|
| | 30 th of August 2015 | | 1 st of August 2016 | |
| | PA | UA | PA | UA |
| Water | 100.0 | 100.0 | – | – |
| OA | | 95.6 | | 96.5 |
| K | | 92.5 | | 94.6 |

1.15% of forest canopy gaps, and 0.25% of water. More in details, the core area consists mainly of forests (92.49%) while grasslands dominate (59.92%) in the buffer zone (Fig. 2). The inner part of the core area is dominated by coniferous trees while the surrounding area is dominated by mixed forest of beech-fir-spruce and by pure beech stands (Fig. 2). Forest canopy gaps were mainly found in conifer-dominated areas (99%).

Within the reserve area, 2638 forest canopy gaps were detected that cover a total of 67.95 ha, resulting in a gap fraction of 0.93% and a gap density of 0.45 #/ha (Table 4). The average size of gaps is 208.03 m² while the median value is 116.79 m² indicating that the majority of gaps are small, as confirmed by the negative exponential shape of the gaps size distribution (Fig. 3). In particular, 41% of gaps have a surface <100 m²,

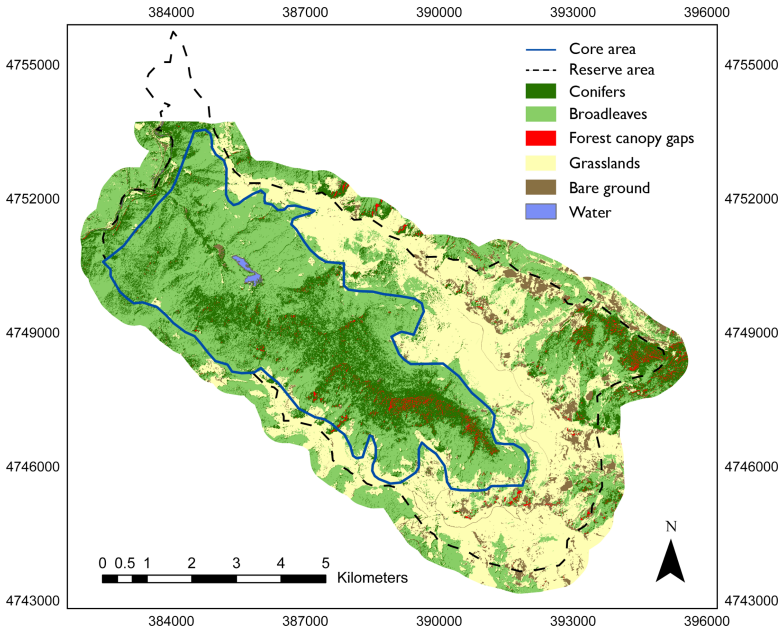


Fig. 2. Classification map of the land-cover classes of the Biogradska Gora National Park. Reference system EPSG:32634 (WGS 84/UTM zone 34N).

35% between 100 and 200 m², 18% between 200 and 500 m², and the remaining 6% are >500 m², whose 2% consists of gaps >1000 m² and only 0.15% are gaps >5000 m².

The core area and the buffer zones did not differ in terms of size (area), shape (perimeter), and frequency distribution of gaps (Table 4). On the other hand, the abundance of gaps was two times higher in the core area than in the buffer zone. However, since the buffer zone is characterized by a high proportion of grasslands (60%), the gap fraction relative to the forest area is higher in the buffer zone (Table 4).

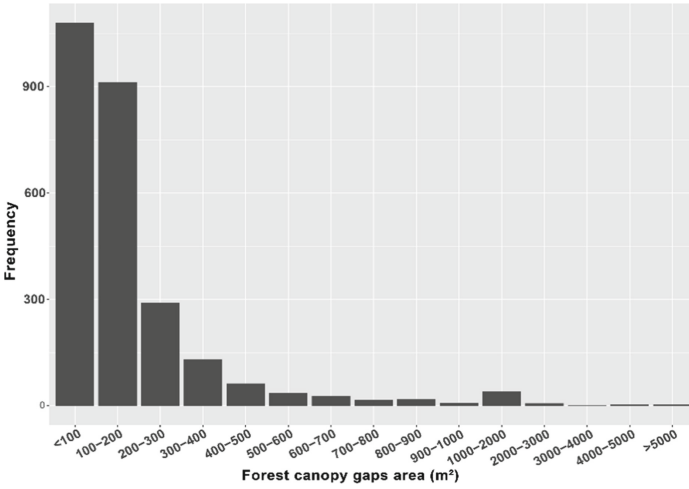


Fig. 3. Distribution of forest canopy gaps according to their size.

Table 4. Landscape metrics and summary of gap attributes in the OGF of Biogradska Gora.

| Variables | Core area | Buffer zone | Reserve area |
|-----------------------------------|-----------|-------------|--------------|
| Total area (ha) | 2834.27 | 3052.66 | 5886.94 |
| Number of gaps (#) | 1674 | 964 | 2638 |
| Density of gaps (#/ha) | 0.59 | 0.32 | 0.45 |
| Mean gap area (m ²) | 210.54 | 203.69 | 208.03 |
| Median gap area (m ²) | 119.78 | 111.85 | 116.79 |
| Mean gap perimeter (m) | 86.34 | 84.36 | 85.62 |
| Median gap perimeter (m) | 60.91 | 57.93 | 59.87 |
| Gap fraction (%) | 1.24 | 0.64 | 0.93 |
| Gap fraction in forest area (%) | 1.34 | 2.01 | 1.53 |

4 Discussion

The Biogradska Gora mixed fir-spruce-beech forest clearly shows old-growthness characteristics. The forest structure and the occurring gap dynamic place the forest among the largest old-growth forest remnants in South-Eastern Europe.

The combination of textural metrics with spectral data during the segmentation process is not a common practice as they are mostly employed in the classification phase [26], even if it has been shown to improve the classification accuracy of the land-cover classes in OBIA [17]. In our case, the use of textural metrics during the segmentation phase (Fig. 4) enhanced the identification of individual tree crowns and forest canopy gaps as they provided proxy information on the vertical forest structure. In fact, the opening procedure allowed us to distinguish between the circular-shaped and well-illuminated crowns of the dominant tree layer and the small trees and shrubs occurring in forest canopy gaps, characterized by lower brightness due to the shadow casted by the surrounding tree crowns.

Forest canopy gaps are more heterogeneous and with a rougher texture than the surrounding tree canopy cover [13, 18]. However, the classification shows lower accuracy in detecting forest canopy gaps compared to the other land-cover classes, as highlighted by a minimum producer's accuracy of 75% and a minimum user's accuracy of 54% (Table 3). The low producer's accuracy associated with forest canopy gaps can be affected by shadows, which we limited by employing the NDVI and the textural metrics in the segmentation and classification phases. Specifically, as a normalized index, NDVI is less affected by the proportion of canopy shadows than single reflectance bands and enhances the distinction between vegetation and bare ground [27].

The category of forest canopy gaps includes openings in the dominant tree canopy cover that can be already occupied by regeneration in various stages of growth. Conventionally, when the infilling trees reach heights equal to half of the height of the surrounding mature trees in the upper canopy [28], the area is assigned to the dominant tree-canopy cover. If the gap is small, the opening can be closed by the lateral growth of the edging tree crowns. This process is particularly evident when broadleaved species are involved, especially beech, since they have higher crown plasticity than conifers [29]. Of all observed gaps, only 1% were detected in broadleaved-dominated stands. This can be partially explained by the capacity of crowns to quickly close the gaps or reduce their size [7, 29]. The majority of gaps (99%) were found in coniferous stands, not only for the absence of lateral crown expansion of spruce and fir, but also since those stands showed the highest OGF characteristics. In OGFs, mortality is mainly occurring at the canopy layer, involving large and old, sometimes even individual, trees [1].

In the Biogradska Gora forest, canopy gaps are most often small (50–200 m²), and large gaps (>1000 m²) are rare (Fig. 3). The large gaps could have been generated by intense windstorm events or most probably by the expansion and fusion of neighboring gaps. This is supported by the shape analysis, which shows that large gaps are characterized by complex and heterogeneous shapes with a large perimeter.

Our analysis suggests that the gap fraction is small (<2%). Such small gap fraction values were also obtained in similar OGFs with remote sensing approaches using very-high-resolution images (Kompsat-2 and WorldView-2) [3, 12]. Such values are consistently lower compared to values derived from terrestrial methods (always >15%)

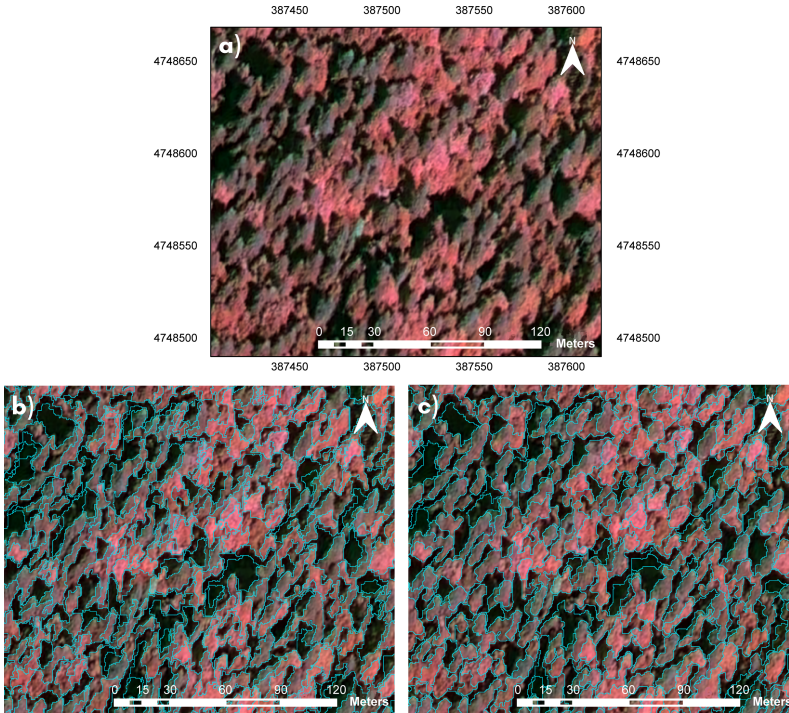


Fig. 4. Detail of the 2015 Pléiades-1B image displayed with false-color composite (R = NIR, G = Red, B = Green): original (a) and segmented either without (b) or with (c) the inclusion of textural information derived using the opening procedure. The parameters used in the Large-Scale Mean-Shift (LSMS) segmentation algorithm were held constant. Reference system EPSG:32634 (WGS 84/UTM zone 34N). (Color figure online)

[7–9]. It thus seems that the classification method substantially underestimates the fraction of the total forest canopy gaps. However, one should bear in mind that a broader range of gap ages and sizes are identified with field surveys [3]. With their finer detail of analysis, field surveys can better detect very small gaps, including those caused by a single tree-death. Moreover, field surveys can better detect old-formed gaps, including those that are almost closed or where regeneration is very high. Instead, the discrimination of gaps with remote sensing methods is hindered by the similar spectral response between the dominant tree canopy cover and the forest canopy gaps [26]. Conversely, remote sensing methods are suitable to detect recently formed gaps and large gaps in which the regeneration has not yet reached great heights or has not completely colonized the gap’s surface. Moreover, remote sensing approaches are suitable to estimate the range of variability of disturbances over large areas. By contrast, terrestrial methods are often limited by the small size of the sampled area [8] and by expensive and time-consuming field inventories, especially in OGFs, which are usually located on steep slopes or in remote areas.

Our study reveals that the analysis of very-high-spatial-resolution satellite imagery alone is not sufficient to map forest canopy gaps and the complex forest structure of mixed

OGFs with high accuracy. Better results could be achieved using stereo-pair images or LiDAR data as they provide canopy heights, thereby allowing a better delineation of gaps [11, 12]. However, these approaches are more expensive due to image acquisition costs, especially in remote areas. Conversely, they achieve substantially higher accuracies (up to 96%) in gap detection [11]. Moreover, recent studies have shown the potential of combining optical and LiDAR data: LiDAR-derived Canopy Height Model allows to better isolate gaps during the segmentation phase. Simultaneously, the synergistic use of the two datasets can result in a more accurate classification map [15].

5 Conclusion

Coupling OBIA and a Random Forest classifier using two very-high-resolution Pléiades images provided high accuracy in mapping most land-cover classes with the exception of the forest canopy gap category. Even if the use of textural metrics during both the segmentation and classification phase enhanced gaps circumscription and the distinction between the dominant and the lower canopy layers, it was however not sufficient to obtain a good accuracy for this class. One reason for the low accuracy could be that the spectral indices (Table 2) derived from Pléiades MS bands (RGB and NIR) tend to saturate in dense vegetation conditions preventing an adequate distinction between young and mature crowns. Another possible reason could be the low number of training samples in the forest canopy gap category, since we used only the objects intersecting our field plot.

A reliable assessment of forest canopy gaps is extremely important to describe the complex forest structure and dynamics of mixed OGFs. Analyses based on single satellite imagery will lack the information on the vertical structure of the forests. Thus, to gain better results in terms of accuracy stereo-pair images, LiDAR data or a combination of optical and LiDAR data may be envisaged as better alternatives.

References

1. Wirth, C., Gleixner, G., Heimann, M. (eds.): *Old-Growth Forests: Function, Fate and Value*. Springer, Heidelberg (2009). https://doi.org/10.1007/978-3-540-92706-8_1. ISBN 978-3-540-92705-1
2. Bauhus, J., Puettmann, K., Messier, C.: Silviculture for old-growth attributes. *For. Ecol. Manag.* **258**, 525–537 (2009). <https://doi.org/10.1016/j.foreco.2009.01.053>
3. Garbarino, M., et al.: Gap disturbances and regeneration patterns in a Bosnian old-growth forest: a multispectral remote sensing and ground-based approach. *Ann. For. Sci.* **69**, 617–625 (2012). <https://doi.org/10.1007/s13595-011-0177-9>
4. Feldmann, E., Drößler, L., Hauck, M., Kucbel, S., Pichler, V., Leuschner, C.: Canopy gap dynamics and tree understorey release in a virgin beech forest, Slovakian Carpathians. *For. Ecol. Manag.* **415–416**, 38–46 (2018). <https://doi.org/10.1016/j.foreco.2018.02.022>
5. Motta, R., et al.: Structure, spatio-temporal dynamics and disturbance regime of the mixed beech–silver fir–Norway spruce old-growth forest of Biogradska Gora (Montenegro). *Plant Biosyst.* **149**, 966–975 (2015). <https://doi.org/10.1080/11263504.2014.945978>
6. Sabatini, F.M., et al.: Where are Europe’s last primary forests? *Divers. Distrib.* **24**, 1426–1439 (2018). <https://doi.org/10.1111/ddi.12778>

7. Bottero, A., et al.: Gap-phase dynamics in the old-growth forest of Lom, Bosnia and Herzegovina. *Silva Fennica* **45**(5), 875–887 (2011). <https://doi.org/10.14214/sf.76>
8. Dröbner, L., von Lüpke, B.: Canopy gaps in two virgin beech forest reserves in Slovakia. *J. For. Sci.* **51**, 446–457 (2012). <https://doi.org/10.17221/4578-JFS>
9. Nagel, T.A., Svoboda, M.: Gap disturbance regime in an old-growth *Fagus-Abies* forest in the Dinaric Mountains, Bosnia and Herzegovina. *Can. J. Forest Res.* **38**, 2728–2737 (2008). <https://doi.org/10.1139/X08-110>
10. Petritan, A.M., Nuske, R.S., Petritan, I.C., Tudose, N.C.: Gap disturbance patterns in an old-growth sessile oak (*Quercus petraea* L.)-European beech (*Fagus sylvatica* L.) forest remnant in the Carpathian Mountains, Romania. *For. Ecol. Manag.* **308**, 67–75 (2013). <https://doi.org/10.1016/j.foreco.2013.07.045>
11. Vepakomma, U., St-Onge, B., Kneeshaw, D.: Spatially explicit characterization of boreal forest gap dynamics using multi-temporal lidar data. *Remote Sens. Environ.* **112**, 2326–2340 (2008). <https://doi.org/10.1016/j.rse.2007.10.001.H>
12. Hobi, M.L., Ginzler, C., Commarmot, B., Bugmann, H.: Gap pattern of the largest primeval beech forest of Europe revealed by remote sensing. *Ecosphere* **6**(5), art76 (2015). <https://doi.org/10.1890/ES14-00390.1>
13. Rich, R.L., Frelich, L., Reich, P.B., Bauer, M.E.: Detecting wind disturbance severity and canopy heterogeneity in boreal forest by coupling high-spatial resolution satellite imagery and field data. *Remote Sens. Environ.* **114**, 299–308 (2010). <https://doi.org/10.1016/j.rse.2009.09.005>
14. Torimaru, T., Itaya, A., Yamamoto, S.-I.: Quantification of repeated gap formation events and their spatial patterns in three types of old-growth forests: analysis of long-term canopy dynamics using aerial photographs and digital surface models. *For. Ecol. Manage.* **284**, 1–11 (2012). <https://doi.org/10.1016/j.foreco.2012.07.044>
15. Yang, J., Jones, T., Caspersen, J., He, Y.: Object-based canopy gap segmentation and classification: quantifying the pros and cons of integrating optical and LiDAR data. *Remote Sens.* **7**, 15917–15932 (2015). <https://doi.org/10.3390/rs71215811>
16. Zielewska-Büttner, K., Adler, P., Ehmann, M., Braunisch, V.: Automated detection of forest gaps in spruce dominated stands using canopy height models derived from stereo aerial imagery. *Remote Sens.* **8**, 175 (2016). <https://doi.org/10.3390/rs8030175>
17. Hossain, M.D., Chen, D.: Segmentation for Object-Based Image Analysis (OBIA): a review of algorithms and challenges from remote sensing perspective. *ISPRS J. Photogramm. Remote Sens.* **150**, 115–134 (2019). <https://doi.org/10.1016/j.isprsjprs.2019.02.009>
18. Nyamgeroh, B.B., Groen, T.A., Weir, M.J.C., Dimov, P., Zlatanov, T.: Detection of forest canopy gaps from very high resolution aerial images. *Ecol. Ind.* **95**, 629–636 (2018). <https://doi.org/10.1016/j.ecolind.2018.08.011>
19. Sun, W., Chen, B., Messinger, D.W.: Nearest-neighbor diffusion-based pan-sharpening algorithm for spectral images. *Optical Eng.* **53**(1), 013107-1-013107-2 (2014). <https://doi.org/10.1117/1.OE.53.1.013107>
20. Michel, J., Youssefi, D., Grizonnet, M.: Stable mean-shift algorithm and its application to the segmentation of arbitrarily large remote sensing images. *IEEE Trans. Geosci. Remote Sens.* **53**(2), 952–964 (2015). <https://doi.org/10.1109/TGRS.2014.2330857>
21. Grizonnet, M., Michel, J., Poughon, V., Inglada, J., Savinaud, M., Cresson, R.: Orfeo ToolBox: open source processing of remote sensing images. *Open Geospat. Data Softw. Stand.* **2**(1), 1–8 (2017). <https://doi.org/10.1186/s40965-017-0031-6>
22. Soille, P.: *Morphological Image Analysis: Principles and Applications*, 2nd edn. Springer-Verlag, Heidelberg (2004). ISBN 978-3-642-07696-1
23. Breiman, L.: Random forests. *Mach. Learn.* **45**, 5–32 (2001)

24. Wright, M.N., Ziegler, A.: ranger: a fast implementation of random forests for high dimensional data in C++ and R. *J. Stat. Softw.* **77**(1), 1–17 (2017). <https://doi.org/10.18637/jss.v077.i01>
25. Schliemann, S.A., Bockheim, J.G.: Methods for studying treefall gaps: a review. *For. Ecol. Manag.* **261**, 1143–1151 (2011). <https://doi.org/10.1016/j.foreco.2011.01.011>
26. Kupidura, P.: The comparison of different methods of texture analysis for their efficacy for land use classification in satellite imagery. *Remote Sens.* **11**, 1233 (2019). <https://doi.org/10.3390/rs11101233>
27. Xu, N., Tian, J., Tian, Q., Xu, K., Tang, S.: Analysis of vegetation red edge with different illuminated/shaded canopy proportions and to construct Normalized Difference Canopy Shadow Index. *Remote Sens.* **11**, 1192 (2019). <https://doi.org/10.3390/rs11101192>
28. Tyrrell, L.E., Crow, T.R.: Structural characteristics of old-growth hemlock-hardwood forests in relation to age. *Ecology* **75**, 370–386 (1994). <https://doi.org/10.2307/1939541>
29. Muth, C.C., Bazzaz, F.A.: Tree canopy displacement at forest gap edges. *Can. J. For. Res.* **32**, 247–254 (2002). <https://doi.org/10.1139/x01-196>